JOURNAL OF MATERIALS SCIENCE 25 (1990) 5215–5219

Characterization of fly ash from coal-fired power plants

S. C. WHITE, E. D. CASE
Department of Metallurgy, Mechanics and Materials Science, Michigan State University, East Lansing, MI, USA

X-ray analysis shows that mullite and silica are the major crystalline phases in fly ash. The "method of known additions" from X-ray diffraction techniques was used to calculate changes in the significant peak intensities of mullite and silica to determine their weight fractions in fly ash. This furthers the efforts of characterizing fly ash, which are being conducted to supplement the search for applications of this abundant material. The weight fractions of crystalline mullite and silica were determined to be 14.2 and 5.1 wt%, respectively. Thermal gravimetric studies as well as SEM and particle size analysis were also conducted on the fly ash.

1. Introduction

In 1973 the annual production of fly ash, that material remaining after the combustion of coal, was over 22 million tons [1]. Only about 10% of this was used in concrete and cements [1]. Because of its availability, new uses of fly ash for commerical and industrial applications are being investigated.

The majority of the minerals in coal are classified into one of four groups: aluminosilicates (including clays), carbonates, sulphides, and silica (quartz) [2]. During combustion some minerals such as the clay may be altered thermally, while other minerals, such as the quartz may remain unaltered. The thermally treated coal impurities, along with small amounts of unburned coal, make up the fly ash. The composition of the coal impurities is not fixed, thus composition of the resulting fly ash also varies. The major constituents of fly ash are α-quartz (SiO_2), mullite ($3Al_2O_3 \cdot 2SiO_2$), hematite (Fe_2O_3), magnetite (Fe_3O_4), lime (CaO), and gypsum ($CaSO_4 \cdot 2H_2O$) [3].

Using X-ray diffraction (XRD), Mattigod and Ervin [4] have found that mullite is the dominant crystalline component, followed by minor amounts of quartz for low-density fly ash fractions. Quartz has also been reported as the major crystalline phase in a study of bulk fly ash [5] (no size fractions removed). These results indicate the difficulties in ascertaining general characteristics for a material with such variation.

Mullite does not occur naturally in coal, thus, the mullite observed in the fly ash is assumed to form during combustion by the thermal decomposition of naturally occurring aluminosilicates, such as kaolinite. The decomposition reactions for kaolinite are:

$$Al_2O_3 \cdot 2SiO_2 \cdot 2H_2O \xrightarrow{500°C} Al_2O_3 \cdot 2SiO_2 + 2H_2O$$

$$\text{kaolinite} \longrightarrow \text{metakaolin} + \text{steam}$$

$$3(Al_2O_3 \cdot 2SiO_2) \xrightarrow{980°C} 3Al_2O_3 \cdot 2SiO_2 + 4SiO_2$$

$$\text{metakaolin} \longrightarrow \text{mullite} + \text{silica}$$

Two competing rates determine the amount of mullite formed, the rate of its crystallization from the melt and the rate at which the melt cools to amorphous solidification. The final amount of quartz also depends on these cooling rates because they determine what fraction of SiO_2 (from the metakaolin decomposition reaction) becomes glassy (amorphous) and what fraction crystallizes [6].

2. Experimental procedure

2.1. X-ray analysis

Fly ash and 99.92% pure mullite ($Al_2O_3 \cdot 2SiO_2$) (Baikowski International Corporation, Charlotte, North Carolina) powder were mixed together to make four powder specimens with compositions of 90.0–9.09, 83.3–16.7, 76.9–23.1 and 71.4–28.6 wt % fly ash–mullite. A series of fly ash–99.9% pure silica (Alfa Products, Thiokal/Ventron Division, Danvers, Massachusetts) mixtures were also prepared, with the compositions 90.0–10.0, 80.0–20.0, 70.0–30.0 and 60.0–40.0 wt % fly ash–silica.

The powder masses were determined with a precision of 10^{-6} g using a Sartorius Analytic Electronic Balance. Each specimen (except 100% ash specimen) was mixed using a porcelain mortar and pestle. Comparison of the X-ray diffraction patterns for mixed and unmixed specimens showed no difference in the peak widths, thus confirming that significant particle size reduction did not occur. Peak broadening becomes noticeable for particle sizes smaller than about 40 μm. Though some peak broadening may have been initially present, no change in this effect upon the diffraction patterns was observed for mixed and unmixed ash, thus permitting their comparison in the analyses that follow.

X-ray powder diffraction for all specimens was performed with a General Electric X-ray Diffractometer set at a rate of 500 counts sec^{-1} and a time constant of 1.0. The powder specimen was rotated at a rate of 2° min^{-1} with respect to the incident X-rays. While not

0022–2461/90 $03.00 + .12

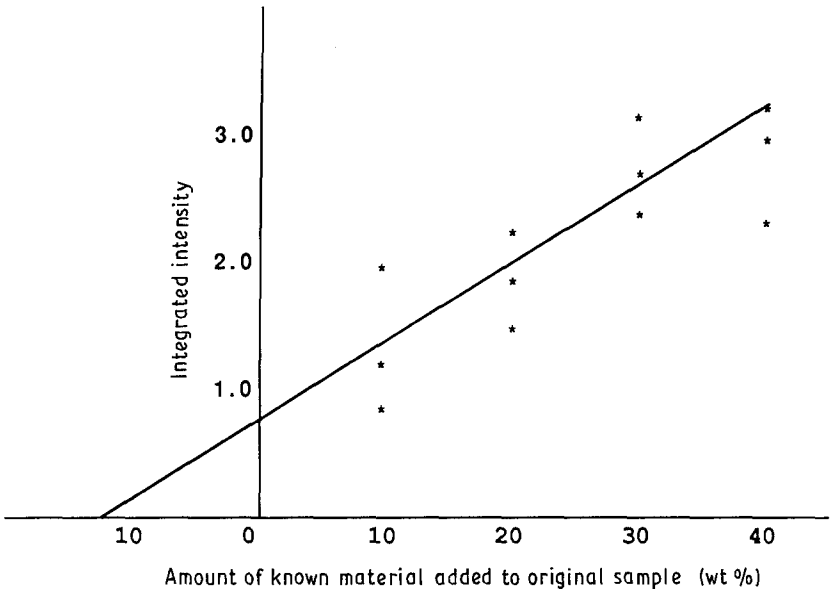

Figure 1 Illustration of the "method of known additions" analysis.

directly measured, the specimen thickness was estimated as 0.1 to 0.2 cm. During compaction of the powder specimens, twisting action was carefully avoided in order to limit particle orientation effects in the specimen. The 2θ ranges of X-ray diffraction were from 15° to 56° for the fly ash–mullite compositions, 15° to 65° for the 100% fly ash, and from 18° to 61° for the fly ash–silica compositions. The X-ray diffraction data for mullite and silica from Brindley [8], along with the diffraction patterns of the mullite and silica standards, were used to identify peaks suitable for analysis in the mullite–flyash and silica–flyash mixtures.

The weight fraction of the mullite and silica phases in the fly ash powders were determined from linear least-squares analyses of the changes in XRD peak intensities and the known amounts of these phases added to the fly ash to induce this change. Central to this procedure is the "method of known additions," an internal standard method of quantitative analysis [8]. If the weight proportion of component C in a powder specimen is sufficiently small or if the mass attenuation coefficients, μ, for the majority of the constituents are similar (i.e. such that μ_2/μ_1 is approximately equal to 1) then, from the method of known additions the weight proportion of C in the original specimen can be expressed by

$$W_c = \frac{W_t(I_1/I_2)}{X + W_t - (I_1/I_2)} \quad (1)$$

where, W_c is the unknown weight fraction of component C, W_t the wt % of pure component C added to mixture, I_1 the intregrated X-ray intensity of the initial specimen, I_2 the integrated X-ray intensity of the mixture and X the mass of the initial specimen.

The calculated mass attenuation coefficients for mullite and silica (Cu$K\alpha$ radiation) are 33.1 and 36.4, respectively [8].

Each 2θ peak identified as a strong diffraction of either mullite or silica in the 100% fly ash pattern was compared to the same peak in the X-ray patterns for the mullite–flyash and silica–flyash mixtures, which contained increasing amounts of their respective standard. To ascertain the effect of the known addition of standard material upon the peak intensity, the outline of the peaks were removed and their masses determined. These mass values constituted the raw data analysed by computer software. Such a mass corresponds to a peak's area, or, integrated intensity. This intensity increases as the quantity of the phase it identifies is increased. An ideal result would be a linear relationship between percent added standard and integrated intensity. To illustrate the method of analysis Fig. 1 shows a plot of integrated intensity against per cent of a phase added to an initial composition. The wt % of the phase in the original specimen is determined by extrapolating to the abscissa, as shown in Fig. 1.

A linear least-squares minimization computer program fits the generated XRD peak intensity data to an equation of the form

$$I = C_1 + C_2X \quad (2)$$

where I is the normalized integrated intensity of the X-ray diffraction peak, C_1 and C_2 are the fitting constants, and X is the wt % of the mullite or silica phase in the original fly ash specimen. The program calculates the fitting constants, the ratio of the constants for $I = 0$, and the correlation coefficient, or, standardized measure of association, r. The analysis may be conducted on the data obtained from an individual 2θ peak, or on any combination of peaks. The wt % mullite or silica in the as-received fly ash can be determined by solving for X when intensity I is zero (Fig. 1). For example, for $2\theta = 42.63°$:

$$C_1 = 0.845$$

$$C_2 = 5.889 \times 10^{-2}$$

$$X(I = 0) = -C_1/C_2 = -14.347$$

which corresponds to about 14.4 wt % in the initial composition.

2.2. Thermal analysis

Thermal analyses of fly ash powder specimens were completed using a Dupont 951 thermogravimetric analyzer (TGA). Fly ash specimens were sealed in aluminium containers approximately 0.5 cm in diameter and 0.2 cm deep. These were heated at various rates to

investigate the presence of volatile species in the fly ash.

2.3. Particle analysis

Separation of particle size ranges was accomplished using US Standard Sieve Series of 100, 150, 200, and 325 mesh sizes stacked in descending order. The fly ash particle size specimens, separated into the standard sieve sizes +100, −100 to +150, −150 to +200, and −200 to +325, were prepared for SEM analysis. (These sizes correspond to +149 μm, −149 to +105 μm, −105 to +75 μm, −75 to +44 μm, and −44 μm, respectively.)

A few drops of water were added to the fly ash powder to create a paste. This paste was applied to a metal plate and surrounded by a brass ring. Buehler Sampl-Kwik Powder and Liquid were mixed and poured into the brass ring to form a sample mount. The electrically non-conductive fly ash was coated with aluminium vapour using a Denton Vacuum DV-502 high vacuum evaporator. Specimens were mounted on to aluminium stubs with silver conductive paint for SEM analysis using an Hitachi S-415 scanning electron microscope.

3. Results and discussion

3.1. X-ray analysis

Relative intensities were measured of the most intense XRD peaks for each of the flyash–mullite and flyash–silica mixtures (Tables I and II).

One peak, $2\theta = 24.00°$, did not match the silica or mullite reference peaks obtained from [8], and was determined to be low tridymite by comparison with diffraction data from [7]. Reconstructive transformations such as high-quartz to high-tridymite which occur at a particular elevated temperature, tend to be much slower than transitions of the displacive type [9]. An example of the latter is high- to low-tridymite, which takes place between the high and low transformation temperatures for this particular structure. At temperatures above 867° C, some of the high-quartz present in the coal under combustion may have transformed reconstructively to high-tridymite. Hence, upon rapid cooling, this small fraction of the silica in the fly ash may have subsequently been "displaced" into a low-tridymite form made possible as a result of the initial reconstructive transformation.

The intensity of the tridymite peak (24.00° 2θ) increased as the wt % of the silica standard increased, indicating that this standard also contained a small fraction of trapped tridymite. This was confirmed with an X-ray diffraction analysis of the standard. Consequently, this peak was used in the silica determination.

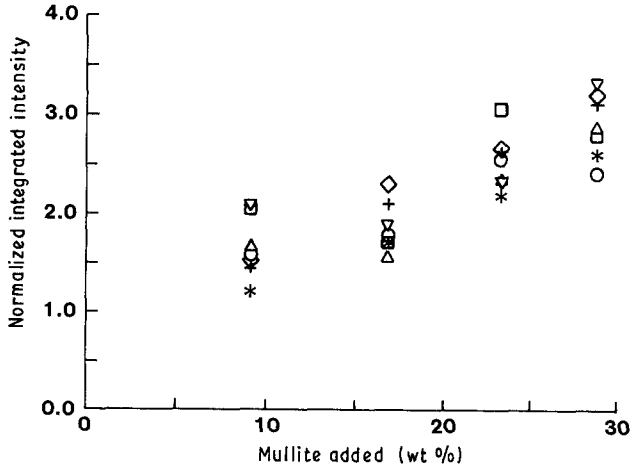

Figure 2 Increases in integrated intensity of mullite X-ray peaks with addition of mullite to initial fly ash powder specimen (*) 42.63, (+) 40.87, (▽) 39.28, (◇) 35.28, (△) 33.24, (□) 30.98, (○) 16.44.

The normalized, integrated X-ray intensities for the flyash–mullite and flyash–silica mixtures are shown in Figs 2 and 3, respectively. The intensities are plotted in correspondence with the wt % of standard added to make the mixture. The linearity discussed earlier is obvious in these empirical results. Not all of the peaks for the flyash–mullite and flyash–silica indicated the expected increases in normalized integrated intensity. In Fig. 2 the peak at $2\theta = 30.90°$ twice showed decreases in the X-ray intensity with respect to the previous peak for increasing mullite, while the 39.28° peak had one such occurrence. The peak at 24.00° 2θ in Fig. 3 displayed a single decrease of intensity with increasing silica addition.

Though these peaks correctly identified the phases being studied, each of these were very small relative to the other 2θ peaks in the analysis. Due to the presence of a "hump" in the fly ash pattern, indicating amorphous phases, peak baselines were estimated from one composition to the next. For the peaks with small areas, the change in integrated intensity, or change in area, resulting from a composition change is more sensitive to the errors in the baseline estimates. This may be the reason for the discrepancies in the flyash–mullite analysis for peaks of 30.98 and 39.28°. The single deviating peak in silica was partially obscured by background and/or minor phase signals. The estimated area may have been greater than that attributable to the 24° tridymite peak. Additionally, as silica was added to the sample, this peak increased in

TABLE I Theoretical 2θ values for X-ray diffraction of mullite with their corresponding correlation coefficients, r

Peak No.	2θ	r
1	16.44	0.960
2	30.98	0.885
3	33.24	0.975
4	35.28	0.996
5	39.28	0.914
6	40.87	0.995
7	42.63	0.980

TABLE II Theoretical 2θ values for X-ray diffraction of silica with their corresponding correlation coefficients, r

Line No.	2θ	r
1	20.85	0.966
2	24.00	0.860
3	36.56	0.805
4	45.80	0.917
5	50.18	0.966
6	59.90	0.995

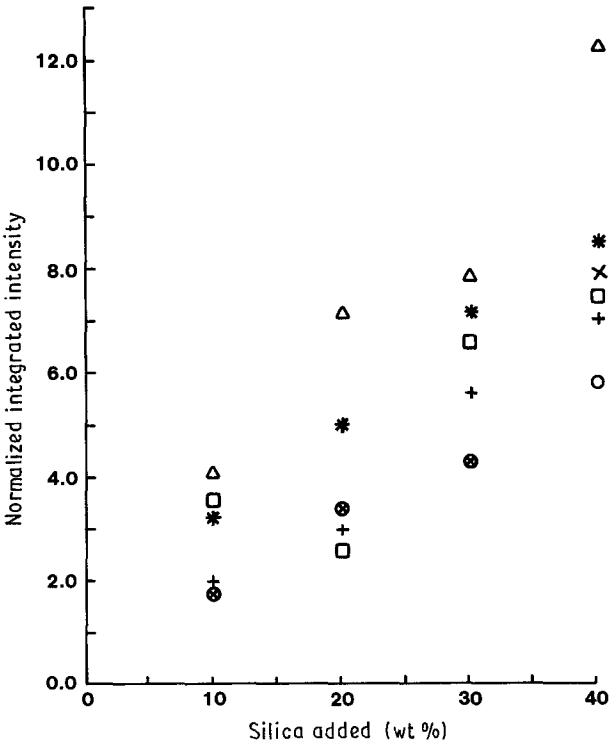

Figure 3 Increases in integrated intensity of silica X-ray peaks with addition of silica to initial fly ash powder specimen (+) 20.85, (□) 24.00, (○) 36.56, (x) 45.80, (△) 50.18, (*) 59.90.

intensity, yet exhibited greater sharpness. This resulted in a decrease in area (integrated intensity) with an increase in added phase. Background effects in subsequent peaks may have been minimized by the increasing size of such peaks.

An additional contribution to deviations from anticipated results is the accuracy with which a diffraction peak can be reproduced. Inherent flaws in the operation of an X-ray diffractometer may also be suspect. XRD beam location, focus, and response to changes in humidity can alter diffraction patterns.

Tables I and II include the individual correlation coefficients, r, for each of the XRD peaks for the mullite and the silica mixtures, respectively. Excluding the r value for $2\theta = 30.98°$ (lowest r) of Table I in the mullite analysis, the least-squares minimization gave (to three significant figures) $C_1 = 0.960$ and $C_2 = 6.64 \times 10^{-2}$, with a correlation coefficient $r = 0.943$ for a total of 30 data points. Excluding $2\theta = 24.00°$ in Table II for the silica analysis, the minimization resulted in the constants $C_1 = 0.845$ and $C_2 = 0.175$, with $r = 0.849$ for 25 data points.

Other peaks with low correlation coefficients may be excluded to improve the correlation in the least-squares analysis. Table III lists the fitting constants and r values for other peak exclusions for the mullite and silica data.

TABLE III Fitting constants, and r values of least-squares minimization for N data points

Material	C_1	C_2	r	N	Excluded peaks
Mullite	0.960	6.64E-2	0.943	30	30.98
Mullite	0.937	6.60E-2	0.954	25	30.98, 39.28
Silica	0.845	0.175	0.849	25	24.00
Silica	1.200	0.226	0.950	10	20.85, 24.00 36.56, 45.80

Averaging the "best fit" calculations resulted in wt % of 14.2 and 5.1 for mullite and silica phases, respectively, in the original fly ash composition. The mullite wt % was determined with 25 data points and exhibited a correlation coefficient $r = 0.954$ while the silica phase quantity was determined using 10 data points which corresponded to $r = 0.950$.

3.2. Thermal analysis

Using the Dupont TGA, a 56.49 mg fly ash powder specimen was heated at 15° C min^{-1} to a maximum temperature of 800° C in air at a flow rate of 100 cm^3 min^{-1}. As indicated by the TGA output, the mass of the fly ash decreased by 3.810% indicating evolution of volatile constituents from the ash. This occurred over the temperature range of approximately 586 to 764° C. At about 800° C most of the volatiles in the ash had been removed.

To determine if chemically or physically absorbed water had volatilized, a specimen of ash was reheated to 900° C for 12 h. The specimen was then exposed to the atmosphere for 1 h. Following this, the fly ash specimen was heated again in the TGA under conditions identical to the procedure described previously. As a final step, the specimen was held for 120 min at 800° C. The resulting TGA graph displayed a horizontal line indicating that the volatiles had been removed by the pre-firing process. If the fly ash had reabsorbed atmospheric water (humidity), it would have contributed to the total weight of the volatilization. The absence of a change in wt % for the second run indicated that the volatiles had been removed by the pre-firing process, and that a large mass fraction of water must not be volatilizing during heating of the ash in the first run. Therefore, the weight loss of 3.81% was determined to be the volatilization of other impurities in the ash.

3.3. Particle morphology and particle size distribution

Figs 4 and 5 are SEM micrographs of the −150 to +200 sieve size (−105 to +75 μm particle size range) at magnifications of 200× and 1200×, respectively. Various features of constituents that exist in fly ash are shown in Fig. 4. Spheres of many different sizes and surfaces are found either loose or embedded in a larger matrix-like structure. At the higher magnification shown in Fig. 5 the matrix appears to be a conglomeration of spherical particles with sizes as varied as those in Fig. 4. Both micrographs provide indication of the complexity of this combustion product.

The separation of particle size ranges was initiated

TABLE IV Particle size distribution of fly ash; individual masses, and wt % of each fraction in total fly ash sample

US Standard Sieve No.	Average diameter (μm)	Mass (g)	% of total
+100	+149	0.2479	0.672
−100 to +150	−149 to +105	1.3084	3.544
−150 to +200	−105 to +75	8.3232	22.540
−200 to +325	−75 to +44	18.0967	49.02
−325	<44	7.5340	20.40

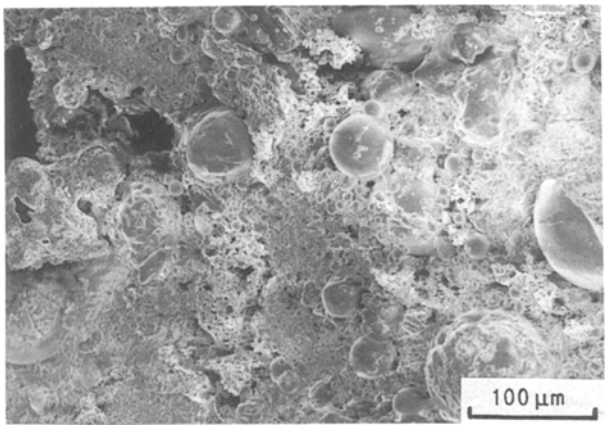

Figure 4 Scanning electron micrograph of fly ash in the particle size range of 75 to 105 μm at magnification $\times 200$.

to attempt to determine which range, if any, contained the greatest mass of fly ash. The percent of total mass values given in Table IV show the largest fraction of fly ash particles have diameters between 44 and 75 μm. Over 70% of the fly ash particles lie within the 105 and 44 μm range. Some deviation must exist for these values due to the conglomeration of some smaller particles. Clustering of the smaller particles was observed in several SEM micrographs of fly ash powder collected in a larger particle size range, thus confirming that such conglomerates may be retained by coarser mesh sizes. Evidence of this can be seen in Fig. 5 when compared to the relative particle sizes of Fig. 4. Several papers exist which address additional questions related to particle size distribution and the distribution of mullite and other crystalline phases with respect to particle sizes in fly ash [3, 4, 10, 11].

4. Conclusion

X-ray analysis of the fly ash powder has shown that mullite and silica are the major crystalline phases in the ash. This is consistent with other studies [3, 4]. The weight fraction of mullite and alpha quartz in the fly ash was 14.2 and 5.1%, respectively. The volatile content (unburned coal, etc.) of the fly ash was 3.81 wt %.

A significant glassy fraction of the fly ash was indicated by the "hump" in the X-ray diffraction pattern 2θ values of approximately 18 to 32°.

The particle size of mullite produced by the decomposition of kaolinite may be as small as 0.01 μm [12]. XRD peaks from particle sizes in the micrometre size are very broad, and in this case such peaks may be at least partially hidden by the broad amorphous hump of the X-ray diffraction pattern. TEM studies could determine the presence and quantities of these phases of possibly microcrystalline mullite in the fly ash.

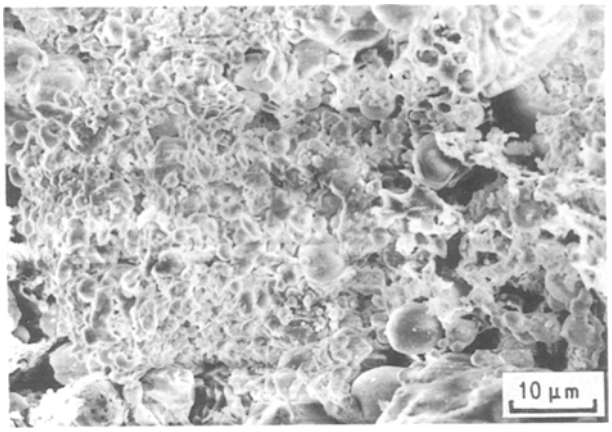

Figure 5 Scanning electron micrograph of fly ash in the particle size range of 75 to 105 μm at magnification $\times 1200$.

Acknowledgement

This work was conducted on fly ash generated by the Lansing Board of Water and Light, Lansing, Michigan. Their financial and professional support during this work was greatly appreciated.

References

1. R. C. JOSHI and E. A. ROSAVER, *Ceram. Bull.* **5** (52) (1973) 456.
2. HAROLD J. GLUSKOTER, "Mineral Matter and Trace Elements in Coal," Coal Structure, Martin L. Gorbaty and K. Ouchi, editors; based on ACS/CSJ Chemical Congress Symposium, April 3–4, p. 3 1979.
3. G. C. FISHER and D. F. S. NATUSCH, *Analytical Methods for Coal and Coal Products* **III** (1979) 489.
4. SHAS V. MATTIGOD and JAREL O. ERVIN, *Fuel* August (1983) 927.
5. BARRY E. SCHEETZ and WILLIAM B. WHITE, "Characterization of Crystalline Phases in Fly Ash by Microfocus Raman Spectroscopy." *Mat. Res. Soc. Symp. Proc.* Vol. 43 (Materials Research Society, 1985) pp. 53–60.
6. W. D. KINGERY, H. K. BOWEN and D. R. UHLMANN, "Introduction to Ceramics," 2nd edn (John Wiley and Sons, New York, 1976), Ch. 8.
7. G. BROWN, "Associated Minerals." Crystal Structures of Clay Minerals and their X-ray Identification, Mineralogical Society, Monograph No. 5, 1984 pp. 379 and 404.
8. G. W. BRINDLEY, "Quantitative X-ray Mineral Analysis of Clays." Crystal Structures of Clay Minerals and their X-ray Identification, Mineralogical Society, Monograph No. 5, 1984 p. 418.
9. W. D. KINGERY, H. K. BOWEN and D. R. UHLMANN, "Introduction to Ceramics," 2nd edn (John Wiley and Sons, New York, 1976) Ch. 2.
10. M. W. McELROY, R. C. CARR, D. W. ENSOR and G. R. MARKOWSKI, *Science* **215** (1982) 13.
11. LEE D. HANSEN, DAVID SILBERMANI and GERALD L. FISHER, *Environmental Sci. Technol.* **9** (1981) 1057.
12. W. D. KINGERY, H. K. BOWEN and D. R. UHLMANN, "Introduction to Ceramics," 2nd edn (John Wiley and Sons, New York, 1976) Ch. 7.

Received 6 July
and accepted 1 December 1989